Hindawi
Advances in Civil Engineering
Volume 2018, Article ID 5805294, 9 pages
https://doi.org/10.1155/2018/5805294

Research Article

Identifying the Impact Factors of the Dynamic Strength of Mudded Intercalations during Cyclic Loading

Changbin Yan,[1] **Xiao Xu**,[1] **and Lei Huang**[2]

[1]*School of Civil Engineering, Zhengzhou University, Zhengzhou, Henan 450001, China*
[2]*Department of Engineering Geology and Geotechnical Engineering, Faculty of Engineering, China University of Geosciences, Wuhan, Hubei 430074, China*

Correspondence should be addressed to Lei Huang; huanglei@cug.edu.cn

Received 9 May 2018; Accepted 25 July 2018; Published 16 August 2018

Academic Editor: Gaofeng Zhao

Despite reports on previous research associated with the dynamic strength of mudded intercalations during cyclic loading, a systematic investigation of the impact factors of this strength is still valuable. This work aimed at experimentally revealing the impact factors of the strength along with their impacts. The potential impact factors considered in this work include (i) water content, (ii) clay mineral composition, (iii) clay content, (iv) confining pressure, and (v) cyclic failure time. Specimens of mudded intercalations were collected from China and were remolded and prepared for a dynamic triaxial test under cyclic loads. The test results showed that the dynamic strength is impacted by water content (strongly), clay mineral composition (moderately), confining pressure (moderately), and cyclic failure time (weakly); no significant impact of clay content was detected. Moreover, the dynamic cohesion is correlated with clay mineral composition (strongly), water content (moderately), and cyclic failure time (weakly); no significant correlation with clay content or confining pressure was detected. Finally, the dynamic friction angle is correlated with water content (strongly), clay content (moderately), and cyclic failure time (weakly); no significant correlation with clay mineral composition or confining pressure was detected.

1. Introduction

The presence of mudded intercalations is known to deteriorate rock engineering. There exists a limited body of research on the dynamic strength associated with mudded intercalations during cyclic loading. Significant advances in this field include the report by Xue and Wang [1], who determined the dynamic strength indexes of mudded intercalations collected from the Xiaolangdi hydroproject using a cyclic simple shear test and a dynamic triaxial test. However, the potential impact of various factors (e.g., clay mineral composition, water content, grain gradation, and confining pressure) has not yet been reported. Despite numerous previous works investigating the impact factors of the dynamic strength of common fine-grain soils [2–11], little is known as to whether the same impacts occur in mudded intercalations, which are a special soil type whose main mineral composition is clay with breccia and rock fragments.

This work aims at experimentally identifying the impact factors of the dynamic strength of this special soil type and specifying their impacts. The potential impact factors considered in this work include (i) water content, ω, (ii) clay mineral composition, M, (iii) clay content, C, (iv) confining pressure, σ_3, and (v) cyclic failure time, N_f. Test specimens were collected from geological audits that service the large hydroproject near the Hukou waterfall of the Yellow River. Eighty-one groups of specimens with different values of the considered potential impact factors were remolded and prepared for dynamic triaxial testing under cyclic loads. The potential impacts of the factors were investigated and compared with those of related soils.

2. Materials and Methods

2.1. Testing Instrument and Specimens. Dynamic triaxial tests were performed on a DDS-70 electromagnetic vibration

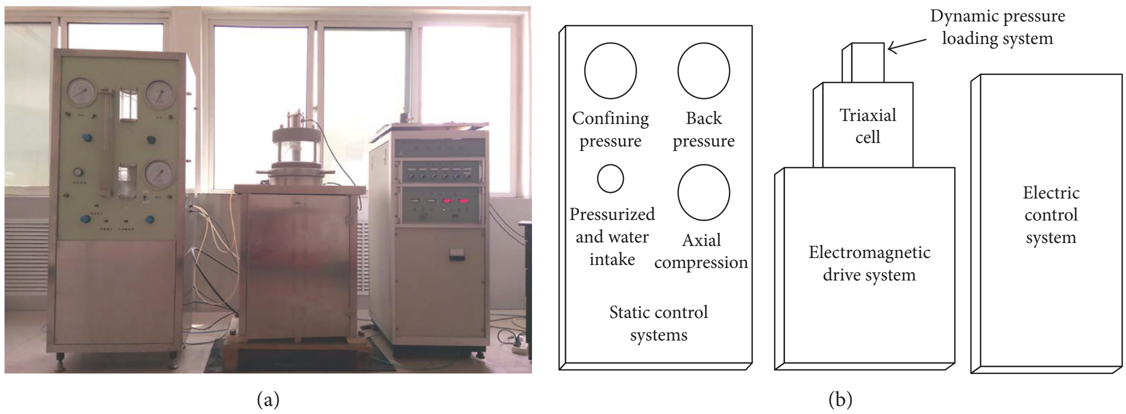

Figure 1: DDS-70 dynamic triaxial test apparatus: (a) view; (b) schematic diagram.

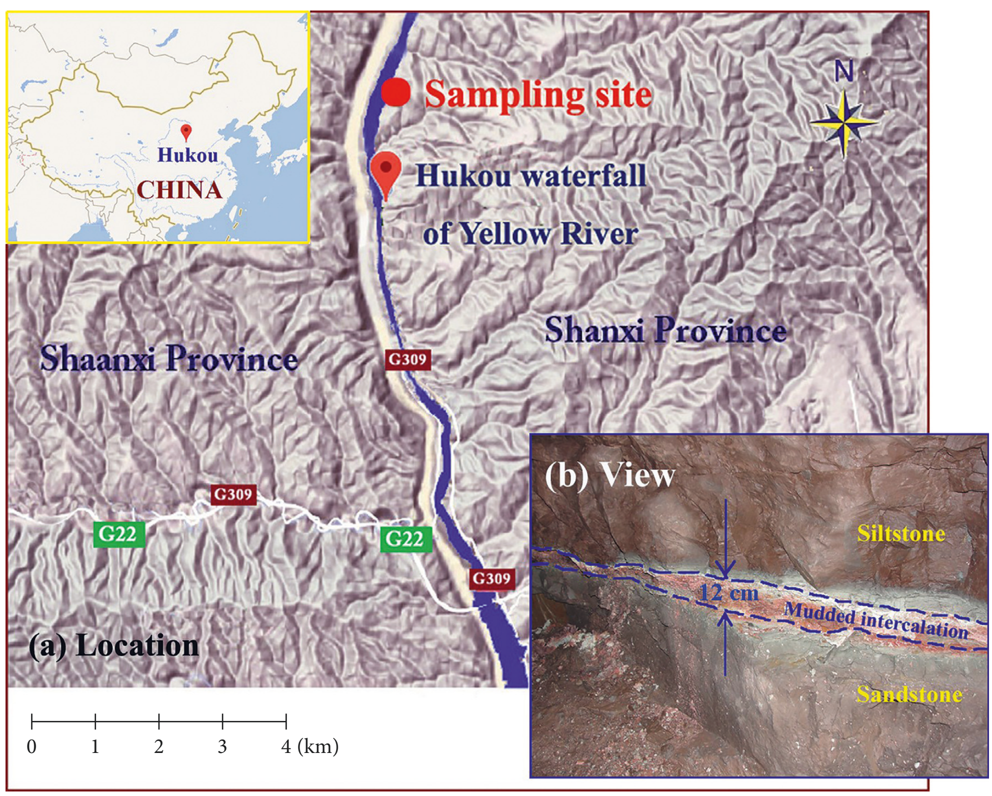

Figure 2: Specimen sampling sites: (a) location; (b) view.

triaxial apparatus, as shown in Figure 1. The maximum allowable axial displacement and maximum allowable axial force are 20 mm and 1370 N, respectively. The allowable frequency range is between 0 Hz and 10 Hz.

The specimens were sampled from a geological audit of a large hydroproject (location shown in Figure 2) and remolded into a standard size (shown in Figure 3). To investigate the potential impacts of (i) water content (ω), (ii) clay mineral composition (M), and (iii) clay content (C) on the dynamic strength and its indexes, specimens with various physical properties, as listed in Table 1, were collected. The grading results of the particle sizes are shown in Figure 4.

2.2. Test Procedure. The test was conducted a total of 81 times. As listed in Table 1, there are 9 groups of remolded specimens for each type of main clay mineral composition. For each group of remolded specimens, 3 levels of confining pressure (σ_3) are applied: 100 kPa, 200 kPa, and 300 kPa. For each level of confining pressure, it is necessary to apply different axial dynamic loads (σ_{de}) to the 3 specimens.

The loading process is shown in Figure 5. An equivalent sinusoidal wave with a frequency (f) of 1 Hz is used as the axial dynamic load, and the consolidation stress ratio (K_c) is set at 1. The test procedure is shown in Figure 6.

In general, under isobaric pressure consolidation, typical soils can be expected to fail once the strain reaches

(a) (b) (c)

Figure 3: Specimens after remolding: (a) Groups 1~3; (b) Groups 4~6; (c) Groups 7~9.

Table 1: Physical properties of remolded specimens.

Group number	Sampling site	Main clay mineral composition, M	Clay content, C (%)	Dry density (g/cm^3)	Water content, ω (%)
1	PD207 and PD302	Mixed montmorillonite/illite	29.2	1.9	11.3
2					15.1
3					18.7
4	PD302	Illite	21.0	1.9	11.3
5					15.1
6					18.7
7	PD207 and PD215	Kaolinite	48.8	1.9	11.3
8					15.1
9					18.7

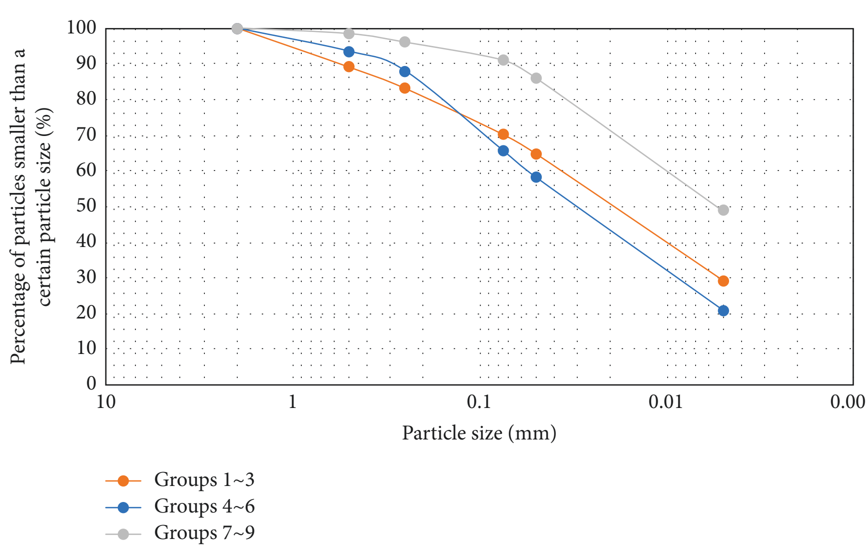

Figure 4: Grading of the particle sizes.

5% [3, 4]. However, the strength of the mudded intercalations tends to be smaller in comparison with common soils. As a result, under cyclic loading, the initial strain values are larger and the development of damage is slower. This 5% strain failure criterion is therefore not quite suitable for mudded intercalations. Instead, the 10% strain failure criterion [12] is more reasonable and was therefore adopted in the test.

3. Results

3.1. Properties of Dynamic Strength, τ_{df}. The cyclic time corresponding to the time point at which the cumulative strain (ε_d) meets the prescriptive strain failure criterion is defined as the cyclic failure time (N_f). The dynamic shear stress occurring when the cycle number (N) meets N_f is defined as the dynamic strength (τ_{df}).

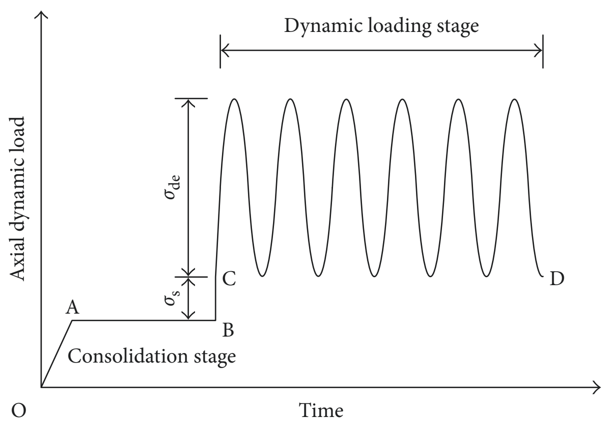

Figure 5: Loading process.

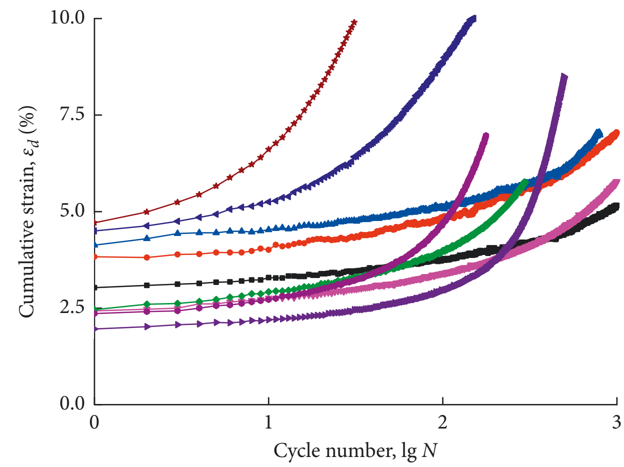

Figure 7: Cumulative strain, ε_d, versus cycle number, N (no. 8 remolded specimens).

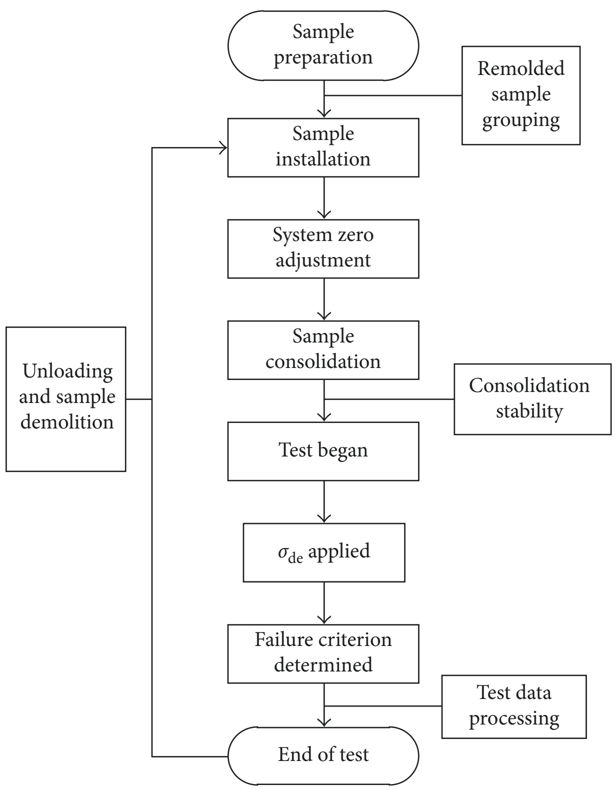

Figure 6: Test procedure.

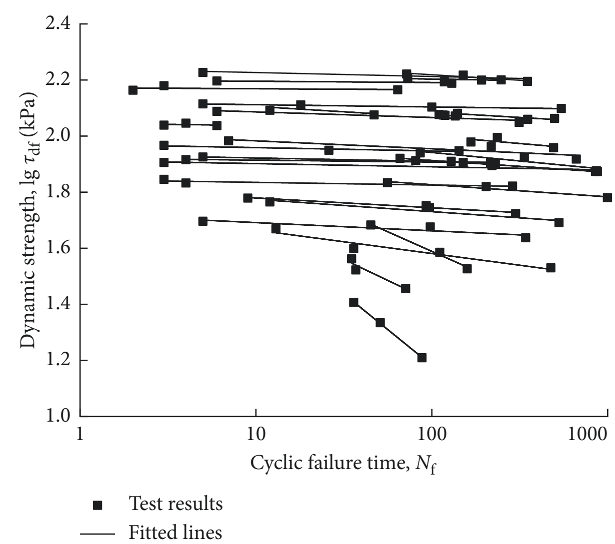

Figure 8: Relationship between τ_{df} and N_f.

Figure 7 shows the relationship between ε_d and N. ε_d initially increases slowly with N, followed by a more rapid increase. This trend is not affected by the confining pressure, σ_3. Moreover, the increase of σ_3 and the cyclic stress ratio (r_d; $r_d = \sigma_{de}/\sigma_3$) contribute to an increased initial cumulative strain value (ε_0), an increased rate of ε_d, and a decreased N_f.

The relationship between τ_{df} and N_f is shown in Figure 8.

As shown in Figure 8, τ_{df} decreases with N_f. Their relationship is fitted as

$$\tau_{df} = A N_f^{-B}, \quad (1)$$

where A and B are fitted coefficients.

The obtained values of A and B are listed in Table 2. More than 63% of the R^2 values are greater than 0.7, indicating a good fit.

An orthogonal test [3] (Table 3) shows that A is impacted by M (strongly), σ_3 (moderately, positive), and ω (weakly, initially negative and then positive). The B is impacted by ω (strongly, positive), M (slightly), and σ_3 (weakly, negative).

3.2. Impact Factors of Dynamic Strength, τ_{df}. The orthogonal test results show that τ_{df} is correlated with ω (strongly), M, σ_3 (moderately), and N_f (weakly). Figure 9 shows τ_{df}~N_f under different conditions, while Figure 10 shows the impact of factors on τ_{df}, where the ordinate is $k_{jm}/k_{jm\max}$ and the abscissa is the impact of the factors.

3.2.1. Impact Factor I: Water Content, ω. Figure 9(a) indicates that τ_{df} decreases with ω when the main clay mineral composition is kaolinite and σ_3 is 200 kPa. In comparison,

Table 2: Obtained values of A and B.

Group number	Confining pressure, σ_3 (kPa)	A	B (10^{-2})
1	100	6.324	0.947
	200	7.736	0.817
	300	8.779	0.353
2	100	6.138	3.498
	200	7.175	1.174
	300	8.533	3.822
3	100	9.035	50.931
	200	7.441	29.820
	300	8.554	27.871
4	100	6.774	1.127
	200	8.899	5.376
	300	9.236	0.989
5	100	6.916	1.195
	200	8.332	0.807
	300	9.947	3.927
6	100	6.776	4.332
	200	7.869	6.066
	300	8.231	5.375
7	100	6.828	0.678
	200	8.660	3.690
	300	9.025	0.444
8	100	7.372	4.224
	200	7.474	2.838
	300	8.217	1.994
9	100	5.746	8.360
	200	5.588	2.914
	300	6.164	4.403

Table 3: Orthogonal test results. K_{jm} is the sum of the parameters for the row level m repeated tests for the j line factor. k_{jm} is the average value of the parameters. R_j is the range (i.e., the difference between the maximum and minimum) of k_{jm}. $\eta_j = (R_j/\sum R_j) \times 100\%$, such that η_j represents the contribution of factor j to A or B.

A	M	ω (%)	σ_3 (kPa)	B	M	ω (%)	σ_3 (kPa)
K_{j1}	25.304	23.800	22.779	K_{j1}	55.570	2.484	52.804
K_{j2}	24.021	22.923	23.079	K_{j2}	8.250	7.855	9.721
K_{j3}	20.466	23.068	23.933	K_{j3}	7.919	61.400	9.214
k_{j1}	8.435	7.933	7.593	k_{j1}	18.523	0.828	17.601
k_{j2}	8.007	7.641	7.693	k_{j2}	2.750	2.618	3.240
k_{j3}	6.822	7.689	7.978	k_{j3}	2.640	20.467	3.071
R_j	1.613	0.292	0.385	R_j	15.773	19.639	14.530
η_j	70.44%	12.76%	16.80%	η_j	31.58%	39.32%	29.09%

τ_{df} initially increases slightly with ω but then decreases (Figure 10(a)). This phenomenon may be attributed to the critical water content, ω_0. That is, for an ω value smaller than ω_0, τ_{df} increases with ω, whereas it decreases for an ω value greater than ω_0. This behavior agrees with findings for common soil reported in [13, 14].

3.2.2. Impact Factor II: Confining Pressure, σ_3. Figure 9(b) shows that τ_{df} increases with σ_3, where ω is 15.1% and the main clay mineral composition is mixed montmorillonite/illite. A similar result is exhibited in Figure 10(c). These results are consistent with those of ordinary soils, as demonstrated in [4, 15, 16].

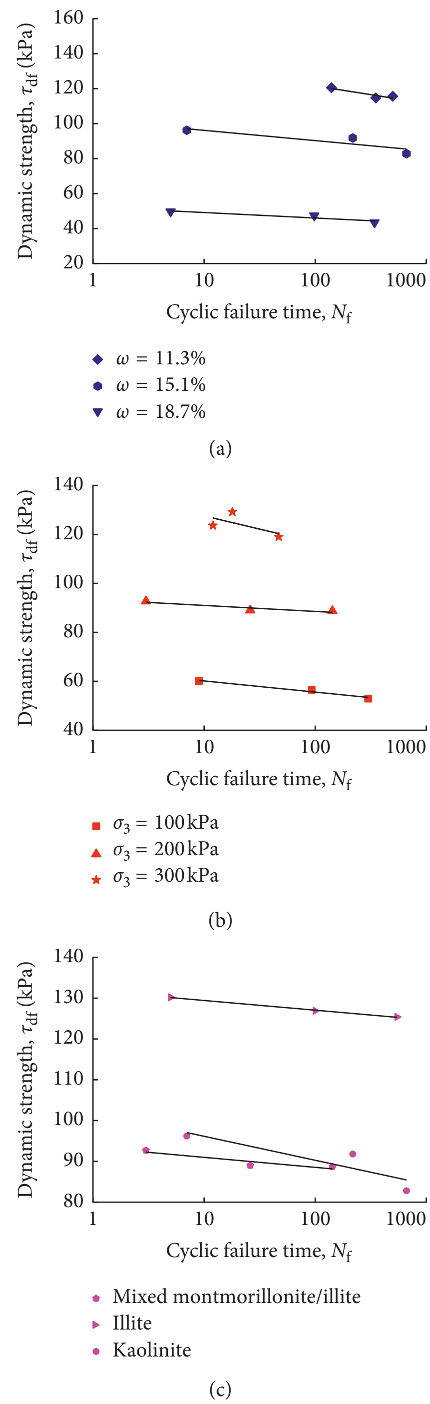

Figure 9: τ_{df} versus N_f for different cases of (a) ω, (b) σ_3, and (c) M.

3.2.3. Impact Factor III: Clay Mineral Composition, M. Figure 9(c) shows τ_{df} when the main clay mineral composition is primarily illite. A similar result is exhibited in Figure 10(b). This result differs from that revealed in [17–19].

3.2.4. Impact Factor IV: Cyclic Failure Time, N_f. Figure 8 shows that τ_{df} decreases with N_f. A different result is presented in Figure 10(d), which shows that τ_{df} does not always decrease with N_f. The difference is likely caused by

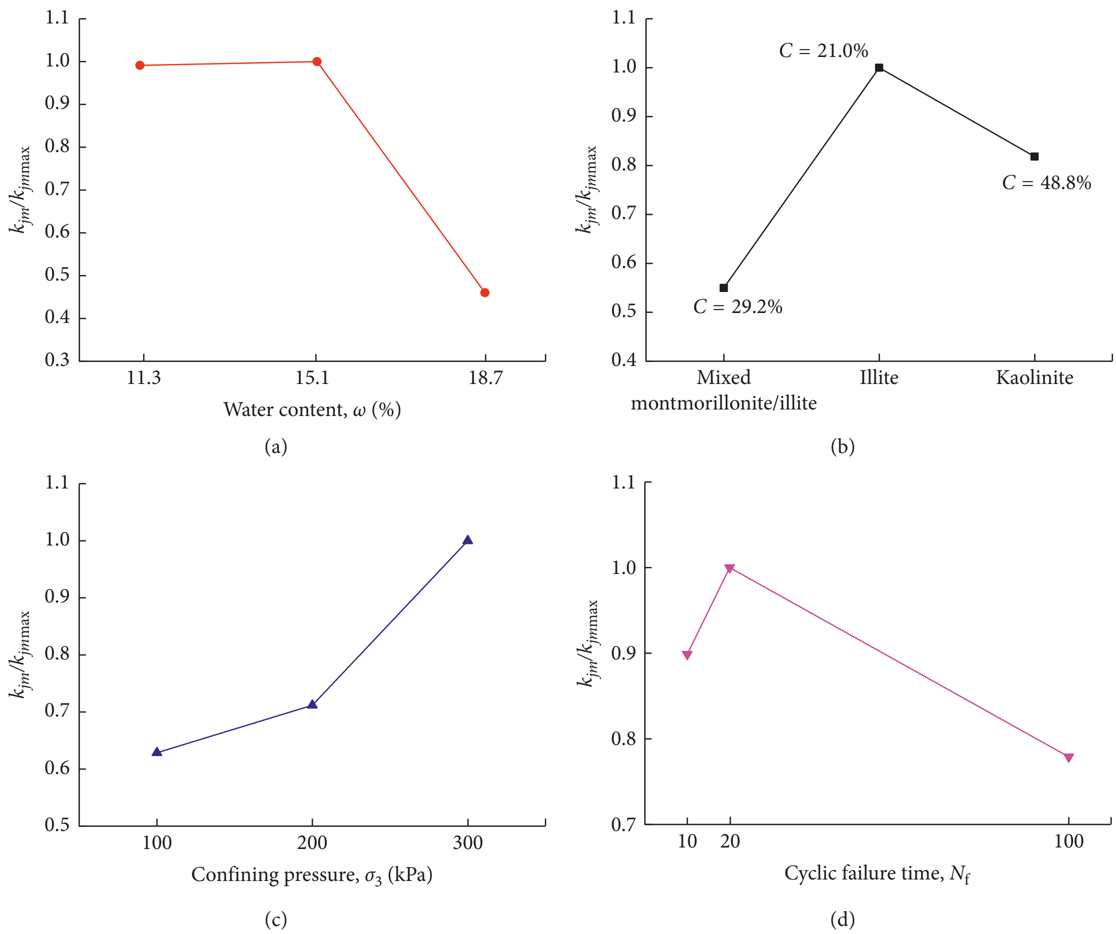

Figure 10: Factor effects on τ_{df}. $k_{jm}/k_{jm\max}$ versus (a) ω, (b) M, (c) σ_3, and (d) N_f.

Table 4: Values of C_d and φ_d determined for the case of $N_f = 20$.

Group number	C_d (kPa)	φ_d (°)
1	11.4	9.6
2	9.8	8.3
3	8.0	3.6
4	15.3	10.2
5	16.5	10.1
6	20.0	6.6
7	19.1	9.2
8	31.3	4.3
9	17.0	2.0

a variation in the compactness. That is, the compactness rises with N_f, resulting in an increase in τ_{df} [5].

3.3. Impact Factors of the Dynamic Strength Indexes, C_d and φ_d. The dynamic strength indexes, C_d and φ_d, are determined as follows: first, τ_{df} is evaluated based on Seed's [20] equivalent cyclic failure time. Then, using τ_{df}, Mohr's stress circle can be obtained, and C_d and φ_d are consequently determined (see results in Table 4). As shown in Table 4, C_d is closely related to the clay mineral composition, which has a contribution rate of 67.23%. φ_d is closely related to ω. Figures 11 and 12 show the impacts of various factors on C_d and φ_d.

3.3.1. Impact Factor I: Water Content, ω. As shown in Figure 11(a), C_d increases with ω when ω is less than ω_0, and vice versa for ω greater than ω_0. φ_d decreases with ω (Figure 12(a)).

3.3.2. Impact Factor II: Clay Mineral Composition, M, and Clay Content, C. Figure 11(b) shows that C_d is affected by the clay mineral composition. Specifically, the C_d values for illite as the main clay mineral composition are greater than those with mixed montmorillonite/illite but lower than those with kaolinite. Moreover, φ_d decreases with C (Figure 12(b)).

3.3.3. Impact Factor III: Cyclic Failure Time, N_f. Figure 11(c) shows that C_d initially increases slightly with N_f and then decreases. A similar variation in φ_d is observed (Figure 12(c)).

3.4. Comparison with Other Soils. The dynamic strength indexes of the mudded intercalations are compared to those of soils from other sites, as documented in [1, 21–23]. The test results are shown in Figure 13.

Figure 13 compares the upper and lower limit values of the dynamic strength for samples from various sites.

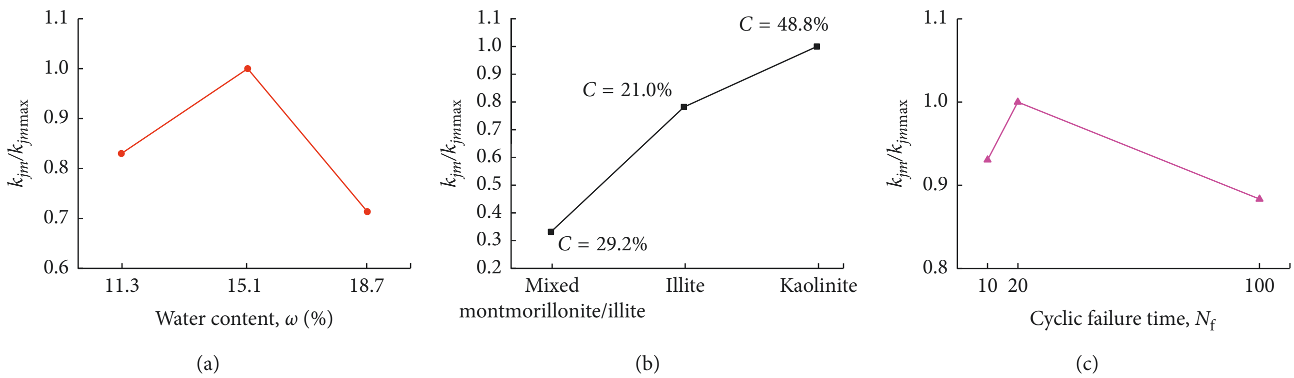

FIGURE 11: Factor effects on C_d. $k_{jm}/k_{jm\max}$ versus (a) ω, (b) M, and (c) N_f.

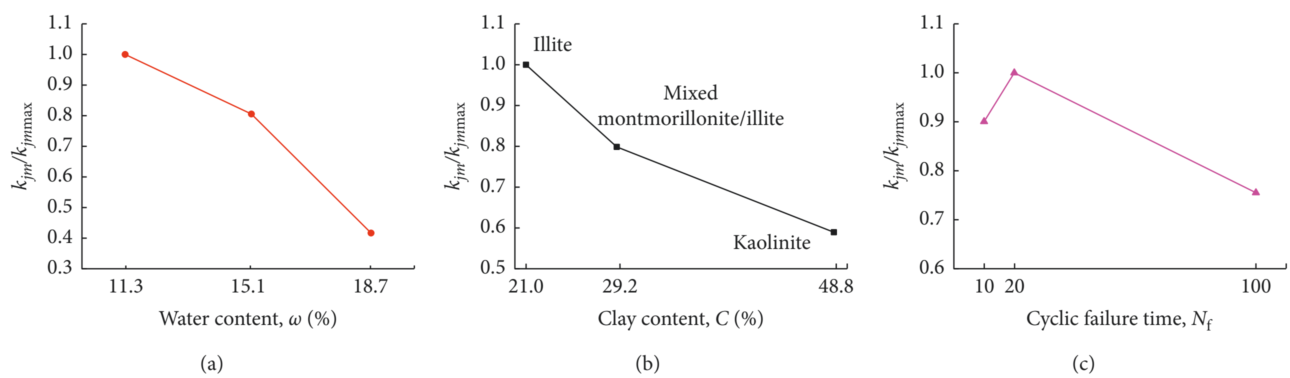

FIGURE 12: Factor effects on φ_d. $k_{jm}/k_{jm\max}$ versus (a) ω, (b) M, and (c) N_f.

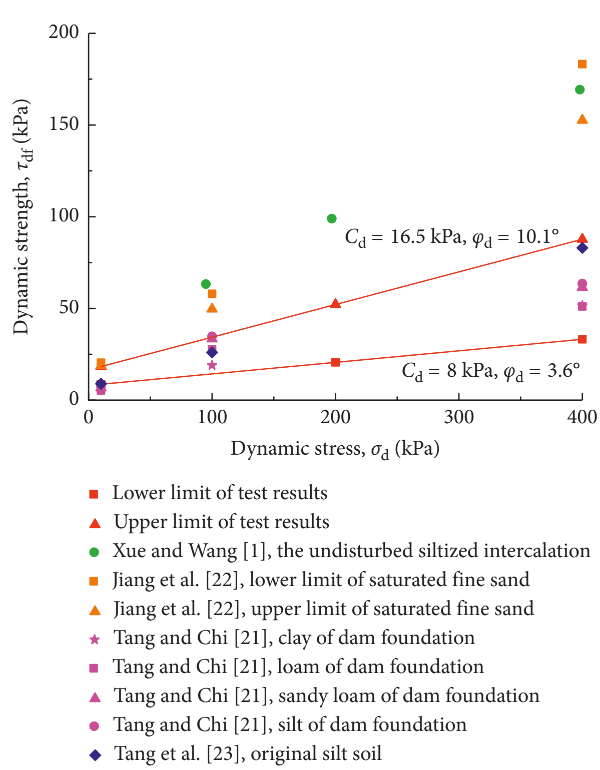

FIGURE 13: Dynamic strength limit of mudded intercalations.

The comparison shows that the dynamic strength of mudded intercalations is generally smaller than that of loess, silt, clay, and other common soils. Possible reasons for this phenomenon are as follows: (a) a structural disturbance due to remolding leads to a significant decrease in the dynamic strength; (b) the mudded intercalations tested in this work are partially composed of mixed montmorillonite/illite, which have relatively low strengths; and (c) the clay content varies depending upon the site, resulting in differences in the dynamic strength.

4. Discussion

Previous literature has concluded that the τ_{df} of mudded intercalations with kaolinite is higher than that for illite [17–19]. However, a different result was observed here; namely, the former is lower than the latter (Figure 9(c)). As a factor that accounts for the disparity between the two results, the clay content of the mudded intercalations in this study corresponding to illite is only 21.0%. This is much lower than the clay content of kaolinite, which reaches 48.8%. The greater the clay content, the smaller the dynamic strength [24–26]. A similar relationship is observed for the dynamic strength indexes of the mudded intercalations, as shown in Figure 11(b). As the mechanical properties of the main mineral composition improve, C_d of the mudded intercalations increases. Moreover, the impact of the clay content on φ_d is more significant, as shown in Figure 12(b), where φ_d decreases with clay content. The clay mineral composition and clay content constitute two primary impact factors for the dynamic strength indexes of mudded intercalations, which are different from common soils.

5. Conclusion

The impacts of various factors on the mudded intercalation dynamic strength, including (i) clay mineral composition, (ii) water content, (iii) clay content, (iv) confining pressure, and (v) cyclic failure time, were investigated. The following conclusions were drawn:

(1) A greater confining pressure and cyclic stress ratio contribute to lower cyclic failure times.

(2) The dynamic strength is strongly impacted by the water content. When the water content exceeds a critical value, the dynamic strength decreases with increasing water content. An opposite variation in dynamic strength with increasing water content is observed when the water content is less than the critical value.

(3) The dynamic strength is impacted by the clay content and clay mineral composition. The strength is correlated with the main clay mineral composition and decreases with the clay content.

(4) The dynamic cohesion is impacted by the clay mineral composition, water content, and cyclic failure time. Specifically, the dynamic cohesion of the mudded intercalations with illite is greater than that for mixed montmorillonite/illite but lower than that for kaolinite. Such cohesions initially increase slightly with water content and cyclic failure time but then decrease.

(5) The dynamic friction angle is strongly impacted by the water content. Specifically, as the water content rises, the dynamic friction angle decreases.

(6) The dynamic strength, cohesion, and friction angle of the mudded intercalations are smaller than those of loess, silt, clay, and common soils.

Data Availability

The data used to support the findings of this study are available from the corresponding author upon request.

Conflicts of Interest

The authors declare that there are no conflicts of interest regarding the publication of this article.

Acknowledgments

This research was financially supported by the National Natural Science Foundation of China (U1504523), the Key Research and Development Plan in Henan Province (182102210014), and the Open Foundation of Jiangxi Engineering Research Centre of Water Engineering Safety and Resources Efficient Utilization (OF201602).

References

[1] S. Y. Xue and S. J. Wang, "Dynamic Triaxial test of the in-situ siltized intercalations in Xiaolangdi project," *Chinese Journal of Geotechnical Engineering*, vol. 19, pp. 89–94, 1997.

[2] W. P. Gong, Y. M. Tien, C. H. Juang, J. R. Martin, and J. Zhang, "Calibration of empirical models considering model fidelity and model robustness—focusing on predictions of liquefaction-induced settlements," *Engineering Geology*, vol. 203, pp. 168–177, 2016.

[3] D. Q. Li and E. T. Selig, "Cumulative plastic deformation for fine-grained subgrade soils," *Journal of Geotechnical Engineering*, vol. 122, no. 12, pp. 1006–1013, 1996.

[4] D. W. Li and J. H. Fan, "A study of mechanical property of artificial frozen clay under dynamic load," *Advances in Civil Engineering*, vol. 2018, Article ID 5392641, 8 pages, 2018.

[5] E. Cowgille, A. Yin, T. M. Harrison, and X. F. Wang, "Reconstruction of the Altyn Tagh fault based on U-Pb geochronology: role of back thrusts, mantle sutures, and heterogeneous crustal strength in forming the Tibetan plateau," *Journal of Geophysical Research: Solid Earth*, vol. 108, no. B7, pp. 457–470, 2003.

[6] C. D. Li, J. Yan, J. F. Wu et al., "Determination of the embedded length of stabilizing piles in colluvial landslides with upper hard and lower weak bedrock based on the deformation control principle," *Bulletin of Engineering Geology and the Environment*, pp. 1–20, 2017.

[7] M. Hyodo, A. F. L. Hyde, Y. Yamamoto, and T. Fujii, "Cyclic shear strength of undisturbed and remoulded marine clays," *Soils and Foundations*, vol. 39, no. 2, pp. 45–58, 1999.

[8] Z. Liu, F. Liu, F. Y. Ma et al., "Collapsibility, composition and microstructure of loess in China," *Canadian Geotechnical Journal*, vol. 53, no. 4, pp. 673–686, 2015.

[9] Z. M. He and B. L. Wang, "Instability process model test for bedding rock slope with weak interlayer under different rainfall conditions," *Advances in Civil Engineering*, vol. 2018, Article ID 8201031, 8 pages, 2018.

[10] Y. X. Wang, P. P. Guo, W. X. Ren et al., "Laboratory investigation on strength characteristics of expansive soil treated with jute fiber reinforcement," *International Journal of Geomechanics*, vol. 17, no. 11, article 04017101, 2017.

[11] X. G. Wang, L. Huang, C. B. Yan, and B. Lian, "HKCV rheological constitutive model of mudstone under dry and saturated conditions," *Advances in Civil Engineering*, vol. 2018, Article ID 2621658, 10 pages, 2018.

[12] ASTM D5311/D5311m-13, *Standard Test Method for Load Controlled Cyclic Triaxial Strength of Soil*, ASTM International, West Conshohocken, PA, USA, 2013.

[13] J. Li, S. X. Chen, and L.-F. Jiang, "Test study on the influences of dynamic stress and load history to the dynamic properties of the remolded red clay," *Earth Sciences Research Journal*, vol. 20, no. 4, pp. 1–8, 2016.

[14] B. Paramasivam and S. Banerjee, "Factors affecting post-cyclic undrained shear strength of marine clay," *Geotechnical and Geological Engineering*, vol. 35, no. 4, pp. 1783–1791, 2017.

[15] V. Manmatharajan and S. Sivathayalan, "Effect of over consolidation on cyclic resistance correction factors Kσ and Kα," in *Proceedings of Fourteenth Pan-American Conference on Soil Mechanics and Geotechnical Engineering and the Sixty-Fourth Canadian Geotechnical Conference*, Toronto, Canada, October 2011.

[16] H. A. Rondón, T. Wichtmann, T. Triantafyllidis, and A. Lizcano, “Comparison of cyclic triaxial behavior of unbound granular material under constant and variable confining pressure,” *Journal of Transportation Engineering*, vol. 135, no. 7, pp. 467–478, 2009.

[17] H. W. Zhang, Z. J. Wan, D. Ma, B. Zhang, and P. Zhou, “Coupled effects of moisture content and inherent clay minerals on the cohesive strength of remodelled coal,” *Energies*, vol. 10, no. 8, pp. 1234–1241, 2017.

[18] T. C. Kenney, “The influence of mineral composition on the residual strength of natural soils,” in *Proceedings of Geotechnical Conference*, Oslo, Norway, July 1967.

[19] S. Nakamura, S. Gibo, K. Egashira, and S. Kimura, “Platy layer silicate minerals for controlling residual strength in landslide soils of different origins and geology,” *Geology*, vol. 38, no. 8, pp. 743–746, 2010.

[20] H. B. Seed, *Representation of Irregular Stress Time Histories by Equivalent Uniform Stress Series in Liquefaction Analyses*, University of California, California, CA, USA, 1975.

[21] F. Y. Tang and H. Y. Chi, “Dynamic triaxial test on Leizehu reservoir dam,” *Shandong Water Resources*, vol. 16, pp. 40-41, 2015.

[22] J. W. Jiang, X. B. Rao, W. Zhang, J. J. Pan, and Z. B. Wang, “Experimental study on dynamic properties of saturated fine sand in Jingjiang levees,” *China Earthquake Engineering Journal*, vol. 37, pp. 759–764, 2015.

[23] Y. Q. Tang, Y. L. Wang, Y. Huang et al., “Dynamic strength and dynamic stress-strain relation of silt soil under traffic loading,” *Journal-Tongji University*, vol. 32, no. 6, pp. 701–704, 2004.

[24] C. P. Polito and J. R. Martin, “Effects of nonplastic fines on the liquefaction resistance of sands,” *Journal of Geotechnical and Geoenvironmental Engineering*, vol. 127, no. 5, pp. 408–415, 2001.

[25] T. L. Youd, I. M. Idriss, R. D. Andrus et al., “Liquefaction resistance of soils: summary report from the 1996 NCEER and 1998 NCEER/NSF workshops on evaluation of liquefaction resistance of soils,” *Journal of Geotechnical and Geoenvironmental Engineering*, vol. 127, no. 10, pp. 817–833, 2001.

[26] T. Hara, T. Kokusho, and R. Hiraoka, “Undrained strength of gravelly soils with different particle gradations,” in *Proceedings of 13th World Conference on Earthquake Engineering*, Vancouver, BC, Canada, August 2004.